



ELSEVIER

Contents lists available at ScienceDirect

Journal of Luminescence

journal homepage: www.elsevier.com/locate/jlumin

SEM-mapped micro-photoluminescence studies of highly luminescent micro-clusters in erbium-doped silicon-rich silicon oxide

David A. Stanley^a, Hossein Alizadeh^a, Amr Helmy^a, Nazir P. Kherani^{a,b,*}, Li Qian^a, Stefan Zukotynski^a^a Department of Electrical and Computer Engineering, University of Toronto, 10 King's College Road, Toronto, Ont., Canada M5S 3G4^b Department of Materials Science and Engineering, University of Toronto, 184 College Street, Toronto, Ont., Canada M5S 3E4

ARTICLE INFO

Article history:

Received 10 October 2009

Received in revised form

25 June 2010

Accepted 30 August 2010

Available online 8 September 2010

Keywords:

Erbium

Stark

Micro-clusters

Photoluminescence

ErSRSO

SEM

ABSTRACT

This paper reports on the formation of unique micrometer-scale clusters in erbium-doped silicon-rich silicon oxide (ErSRSO) thin films produced by thermal evaporation. Through scanning electron microscopy (SEM) and energy dispersive X-ray spectroscopy (EDX), we identify these micro-clusters as structures where the film curves away from the substrate to encase erbium-rich aggregates. Even though erbium aggregation has been reported to cause quenching, we demonstrate that the micro-clusters as a whole can exhibit significantly enhanced erbium photoluminescence (PL), with emissions over 24 times brighter than the surrounding non-cluster region. Mapping micro-photoluminescence measurements onto SEM images reveals that the erbium aggregates alone do not generate the enhanced PL, but rather the thin film encasing the aggregates is the origin of the emissions. Analysis of the PL Stark splitting shows a correlation between the micro-clusters' fine structure and the strength of their PL. Taken together, the above evidence indicates that the micro-clusters' strong PL is produced by changes in the local environment of the Er^{3+} inside the thin film surrounding the erbium-rich aggregates.

© 2010 Elsevier B.V. All rights reserved.

1. Introduction

Over the last decade, there has been a surge of research in photonics focused on developing high-performance silicon-based light emitters for use in optoelectronic devices. Indeed, the realization of silicon-based photonics could make technologies, such as optical clocks for signal distribution, optical links between microprocessors, and optoelectronic interfacing for fiber-to-the-home communications possible [1]. Erbium-doped silicon-rich silicon oxide (ErSRSO) is of particular interest for both optical amplification and light emission.

Recently, Alizadeh et al. [2] developed a particular sequence of thermal evaporations that produces high photoluminescence yields in ErSRSO samples. The present study focuses on the characterization of micrometer-scale erbium-rich clusters in these samples, which exhibit enhanced photoluminescence (PL).

Erbium aggregation is a common phenomenon in many erbium-doped materials. In silica, it results from lack of non-bridging Si-O^- groups, which causes Er^{3+} to have a very low solubility and to form aggregates once it exceeds a certain critical

concentration [3]. In some cases, the aggregates are large enough to view using an optical microscope [1].

While erbium aggregates are described in the literature, the focus is mainly on their contributions to concentration quenching [3–5]. Most studies of ErSRSO focus on the nanostructure [6–8] rather than the microstructure. The purpose of this study is to show that, although the micro-clusters in our samples contain erbium aggregates, they exhibit the property of enhanced Er^{3+} -related PL emission relative to both the non-cluster regions of the thin film and also to Er_2O_3 powder. The brightest clusters produced emission over 24 times stronger than the surrounding non-cluster regions and over 40 times stronger than pure Er_2O_3 . Thus, these micro-clusters could serve as localized luminescence sources for use in devices, and their mechanism of enhancement may be of interest for optical amplification research. To the best of our knowledge, this is the first time such micro-clusters with enhanced PL have been reported in the literature.

2. Methodology

Thin films of ErSRSO were synthesized on fused quartz substrates by a particular sequence of thermal evaporations, followed by annealing at 1000 °C, as described in detail by Alizadeh et al. [2]. Prior to annealing, the multi-layered thin film composite produced by evaporation had the structure of $\text{SiO}_2\text{-SiO-Er-SiO-SiO}_2$.

* Corresponding author at: Department of Electrical and Computer Engineering, University of Toronto, 10 King's College Road, Toronto, Ont., Canada M5S 3G4. Tel.: +416 946 7372.

E-mail address: kherani@ecf.utoronto.ca (N.P. Kherani).

The layers had a nominal thicknesses of $0.07\ \mu\text{m}$ – $0.03\ \mu\text{m}$ – $0.05\ \mu\text{m}$ – $0.05\ \mu\text{m}$ – $0.10\ \mu\text{m} \pm 5\ \text{nm}$, respectively, as confirmed using a Tencor Alpha-Step 200 Profilometer. Samples were annealed for durations of 1–5 h. While micro-clusters with similar properties were observed for all samples with annealing durations longer than 3 h, the sample annealed for 4 h produced the strongest PL, as discussed in our previous study [2]. Therefore, the sample annealed for 4 h is the subject of this paper.

Micro-photoluminescence measurements were performed using a unique adaptation of the Jovin Yvon Horiba LabRAM HR800 Microsystem in conjunction with a diode-pumped frequency-doubled Nd:YAG excitation laser operating at 532 nm. Samples were mounted in a backscattering configuration. The optical system used a $100\times$ objective lens with a numerical aperture of 0.9, allowing for a laser spot size of $\sim 1\ \mu\text{m}$. To obtain PL data, a kinetic grating with 1200 grooves per millimeter was centered at 520, 660, and 800 nm to provide high spectral resolution recordings in the 540, 660, and 800 nm PL bands, respectively. All sample and Er_2O_3 powder PL measurements were collected under identical acquisition settings. PL enhancement is described by dividing the average cluster PL by that of the non-cluster region. The \pm error values and error bars are expressed as standard deviations.

Optical characterization involved observing the sample through an optical microscope built into the Horiba LabRAM system. Images shown in this paper were recorded using the $100\times$ objective. Scanning electron microscope (SEM) analysis was performed using the Hitachi S-5200 cold field emission scanning electron microscope (FESEM) operating at 10 kV with a beam current of $20\ \mu\text{A}$. Side-on recordings of clusters were obtained by diamond scribing the underside of the sample in a straight line and bending it to the point of fracture, so that break along this line could be obtained. Prior to recording, samples were coated in a carbon paste to improve conductivity.

To obtain SEM-mapped micro-PL data, we utilized the fact that many features on the sample surface are visible using both the optical microscope on the LabRAM system and on the SEM. Therefore, using several clearly identifiable landmarks, we were able to locate the same clusters under both the SEM and optical microscope. When recording PL from these clusters, we saved images showing where the laser was centered and could then greatly magnify these regions using SEM. In some instances, EDX was also cross-correlated with the SEM image.

3. Results

3.1. Physical characterization

Micro-clusters up to $6.75 \pm 0.5\ \mu\text{m}$ in diameter were first observed and characterized using optical microscopy. A representative patch of clusters is shown in Fig. 1. Clusters appear reflective when illuminated from the top and dark when viewed from the bottom, indicating they are composed of opaque and reflective material in the visible spectral region.

Fig. 2A presents a cluster viewed from the side using SEM in secondary electron (SE) mode, and reveals that micro-clusters are regions where part of the thin film is displaced to form a hollow shell with crystals located on the inside layer. As discussed later, these crystals also appear prominently in the top-down view presented in Fig. 6B. Fig. 2B shows the same region of the sample with the SEM in backscatter mode; superimposed is an EDX line scan that measures atomic composition. In the backscatter image, bright pixels represent regions with a high atomic number density. Since erbium is the only element used in the evaporation with a high atomic number, this is a strong indication that these crystals are erbium-based. This is corroborated by the fact that the EDX line scan shows an increase in erbium and a drop in silicon levels. The above findings match the description of rare-earth ion aggregation provided in the review by Kenyon [1]. Taken together, the above evidence provides a strong indication that clusters are elevated regions of the thin film containing erbium-rich aggregates in their centres.

Other features in the SEM images include an erbium-rich band that is present throughout the sample, in both the cluster and non-cluster (Fig. 2D) regions, and is likely leftover from the initial deposition. We would expect the darker material above and below the erbium-rich regions to be SiO_x from the original deposition. However, there are also light globules as much as 100 nm in diameter suspended in the SiO_x (Fig. 2B), which are most likely small globules of erbium that have drifted away during annealing and represent mixing within the system. When observing from above, these globules appear to be present in both the cluster and the non-cluster regions; however they become smaller near the cluster borders (Fig. 2C). While these globules clearly form above the erbium-rich regions, it is unclear the extent to which they are present below.

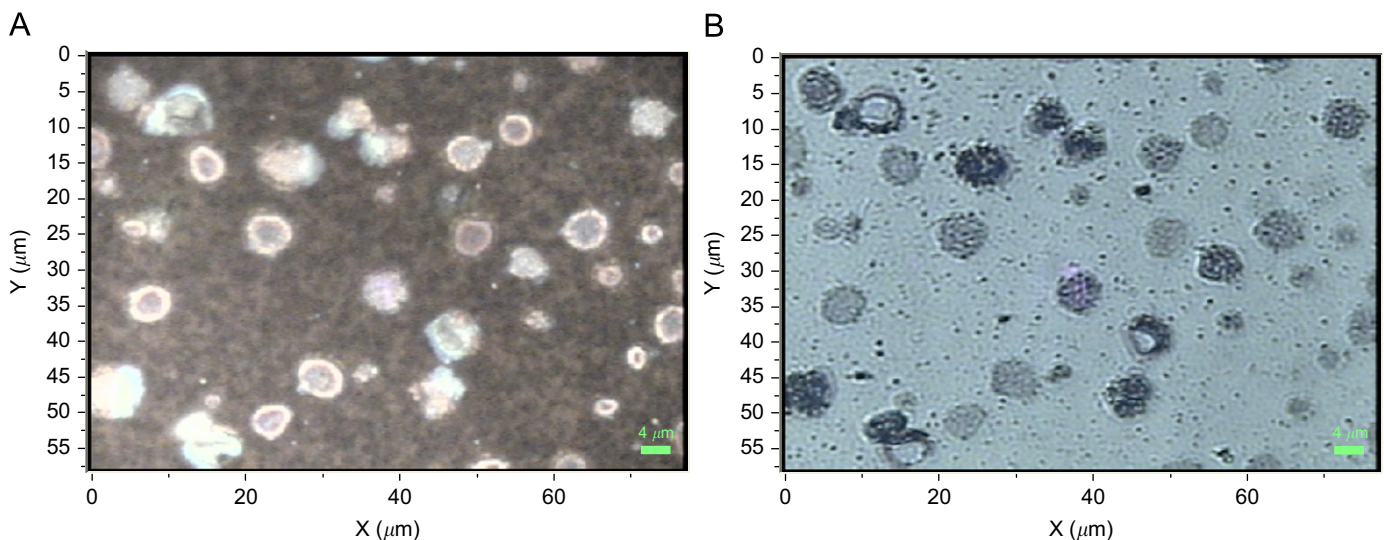


Fig. 1. Physical characterization of erbium micro-clusters. (A) Optical images of clusters taken from Sample 98 using top-down illumination. (B) Same as (A), except using bottom-up illumination. Taken together, these two images indicate that erbium clusters are made of a substance that is both reflective and opaque.

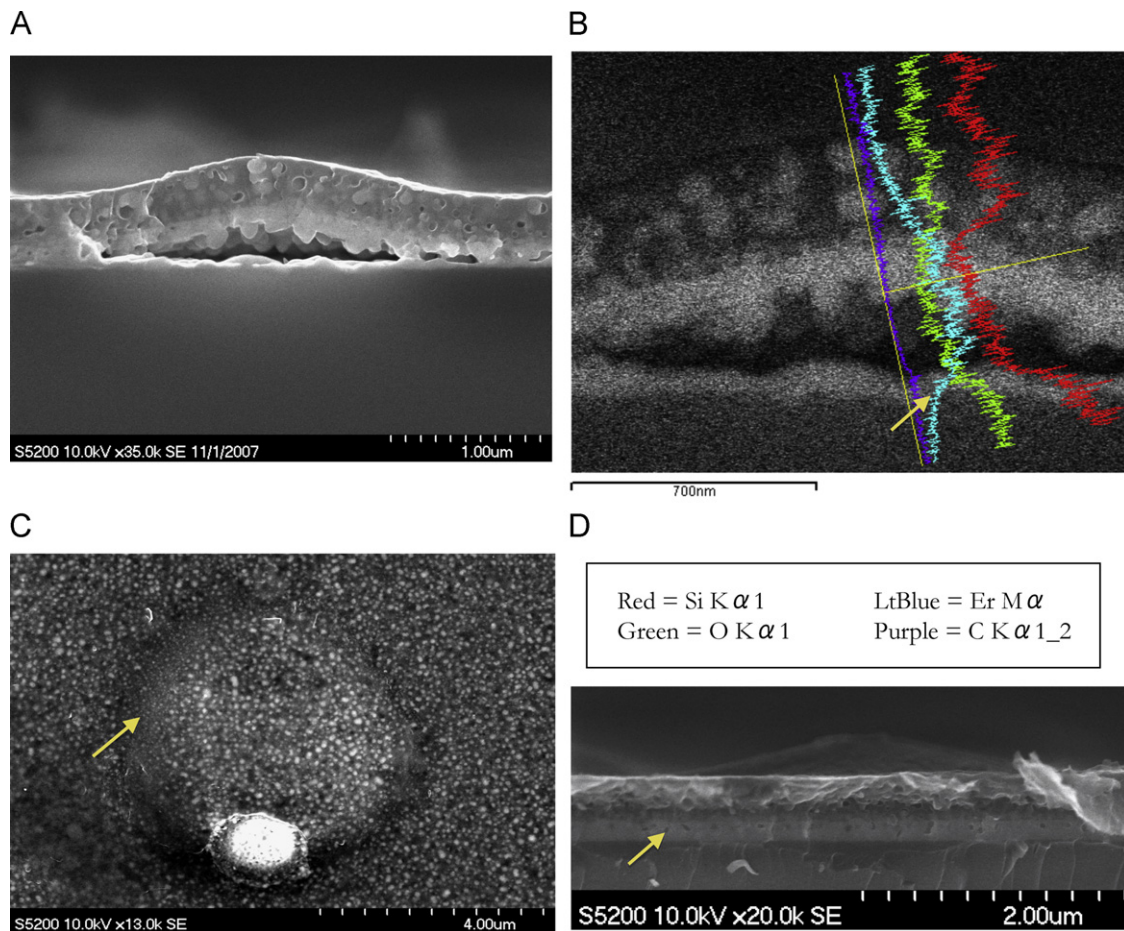


Fig. 2. (A) Side-on SEM SE image of a typical cluster. (B) SEM backscatter and EDX line scan of the same cluster. The crystalline region in the centre appears bright in the backscatter image, indicating a high concentration of erbium. This is corroborated by the EDX line scan of elemental composition (see legend). The backscatter image also shows that erbium from the erbium layer has diffused upwards through the film in small globules as much as 100 nm in diameter. (C) Top-down SEM SE of a single Type 1 cluster, illustrating variations in globule size near cluster edges. (D) Side-on SEM of non-cluster region, which also contains the remnants of the erbium layer from the original deposition (light band).

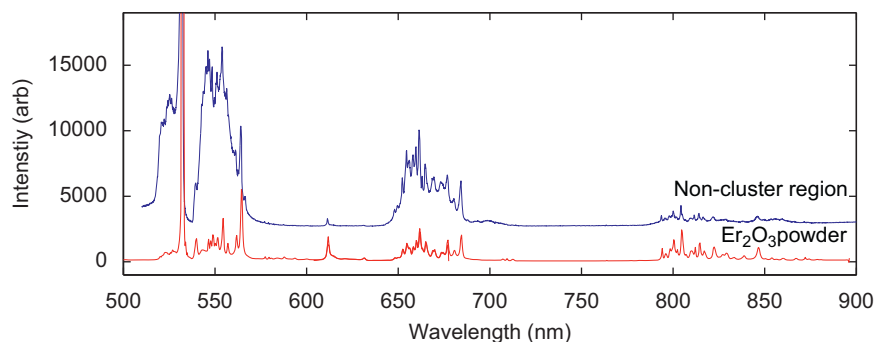


Fig. 3. Comparison of the PL spectrum of the non-cluster region with that of erbium (III) oxide powder. A correspondence exists amongst major PL bands at 540, 660 and 800 nm. The cluster and non-cluster regions for all annealing durations exhibit equivalent emission bands, leading to the conclusion that all major photoluminescence originates from erbium ions.

3.2. Optical characterization

3.2.1. Photoluminescence bands

Fig. 3 illustrates the PL of the regions of film between the clusters (henceforth termed the non-cluster region; see Fig. 1) as compared to the PL of erbium (III) oxide powder (Er_2O_3). All the major PL bands match, indicating that the PL originates from the same source, namely radiative intra-4f transitions in Er^{3+} ions. The 540 nm band corresponds to the $^4\text{S}_{3/2} \rightarrow ^4\text{I}_{15/2}$ erbium

transitions; the 660 nm band corresponds to the $^4\text{F}_{9/2} \rightarrow ^4\text{I}_{15/2}$ transitions; and the 800 nm band corresponds to the $^4\text{I}_{9/2} \rightarrow ^4\text{I}_{15/2}$ transitions [9]. Furthermore, the emission band at wavelengths below 532 nm is likely associated with the $^2\text{H}_{11/2} \rightarrow ^4\text{I}_{15/2}$ transition. The fact that it is at a higher energy than the excitation line can likely be attributed to thermal effects. While the PL spectrum of the non-cluster is shown here, repeated measurements from both the non-cluster and non-cluster regions of all samples revealed that PL emission was consistently restricted to the same bands.

This provides conclusive evidence that the PL measured from our samples is erbium-based.

3.2.2. Stark splitting

PL from both the cluster and the non-cluster regions are shown to exhibit fine structure in the emission spectrum that can be attributed to a combination of the Stark splitting and broadening. PL from the clusters themselves exhibit several different types of fine structure that are different from the standard set of peaks present in Er_2O_3 . A pattern in these observations exists: measuring PL from 48 randomly selected clusters allowed us to group clusters with a similar fine structure into three discrete types (Types 1–3). Four randomly selected spectra of each type are presented in Fig. 4. Note that, for simplicity of presentation, only the 540 nm band is shown in Fig. 4; however, similar categorization is possible using the fine structure of the 660 and 800 nm bands.

The three types of cluster spectra were classified based on the following qualitative features: Type 1 spectra have two broad peaks at 546 and 556 nm, and a number of smaller crests riding on top of these peaks. Type 2 clusters have very well defined Stark peaks that are distinctly different from those of the non-cluster region and Er_2O_3 powder. Type 3 clusters have two broad peaks, but, unlike Type 1, the peak centered at 556 nm is markedly larger than the one at 546 nm. They are also rounder and contain fewer

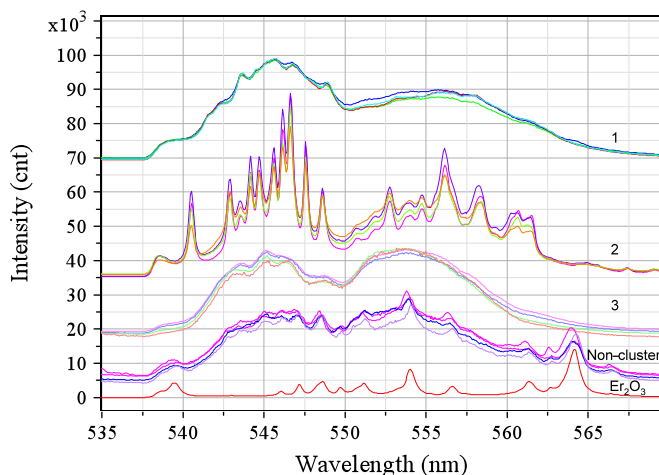


Fig. 4. PL fine structure of the 540 nm band. Spectra from four randomly selected clusters of each type (Types 1–3) are shown, in order from top to bottom. The non-cluster and Er_2O_3 spectra are shown for comparison. There are strong differences between clusters of different types, but very low variability on a cluster-to-cluster basis within the same class. Intensities of each spectrum have been normalized and scaled and are measured in arbitrary units.

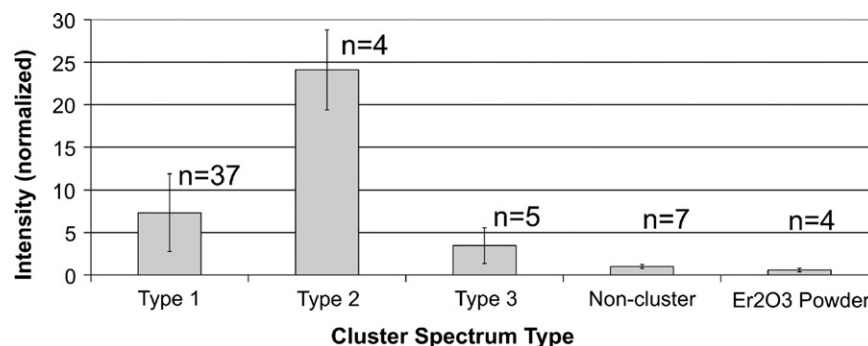


Fig. 5. Intensity of 540 nm PL band as a function of cluster type. Integrated μ -PL intensity from a random selection of clusters is shown to be many times larger than that of the non-cluster region and of Er_2O_3 powder. The spectrum was integrated from 536 to 570 nm, and the number of clusters of each type is reported. Error bars represent standard deviation, thereby providing estimates of the cluster-to-cluster intensity variation.

distinct crests. Sampling the non-cluster region consistently produced spectra that have the same set of peaks as Er_2O_3 , and also an underlying broadening. Of the 48 clusters examined and classified, two clusters emitted spectra that appeared to be a mixture of multiple cluster types, while the rest fit well into the above classification scheme.

3.2.3. Correlation between fine structure and cluster PL intensity

The classification of spectra into various types based on Stark splitting is relevant because a strong correlation exists between the appearance of the fine structure and the cluster's PL brightness. This is illustrated in Fig. 5, which shows the integrated PL intensity of the 540 nm PL band as a function of cluster spectrum type. Note that although only the 540 nm band is shown for purposes of brevity, additional measurements (not shown) have confirmed that the 660 and 800 nm bands are proportional. Thus, while we have focused on the 540 nm band, the changes in this band's PL are reflected by increases in the 660 and 800 nm bands as well.

Of primary interest is the fact that the Types 1 and 2 clusters are several times brighter than the non-cluster region, which is by itself 2–4 times brighter than the Er_2O_3 powder. Type 2 clusters are the brightest: as seen in Fig. 5, they are 24 ± 5 times stronger than the non-cluster region and are 40 ± 15 times brighter than pure Er_2O_3 powder. Type 3 clusters differ in that they are only marginally brighter than the non-cluster region. They are discussed in the following section.

3.3. SEM-mapped micro-PL characterization:

In the literature, erbium aggregates are said to quench PL, which appears to contradict our findings of PL enhancement. However, it is possible that the increased PL is independent of the erbium aggregates and, rather, the increase comes from the deformed portion of the thin film as shown in Fig. 2A.

We tested this hypothesis by using top-down SEM to identify a number of clusters with erbium aggregates visible from above. PL measurements revealed that these aggregates have the same Stark splitting as Type 3 clusters. Conversely, clusters with the thin film still intact were found to express the high intensity Type 1 or 2 PL spectra. These results are best illustrated by the cluster shown in Fig. 6B, which exhibits both an erbium crystalline region and a partially intact thin film region present in the same cluster. The corresponding PL spectra in Fig. 6C shows that the crystalline regions have lower intensity emissions with the rounded peaks characteristic of Type 3 clusters, while the region where the thin film is still intact displays a high intensity Type 2 spectra. Likewise, Fig. 6A shows a typical cluster with the thin film

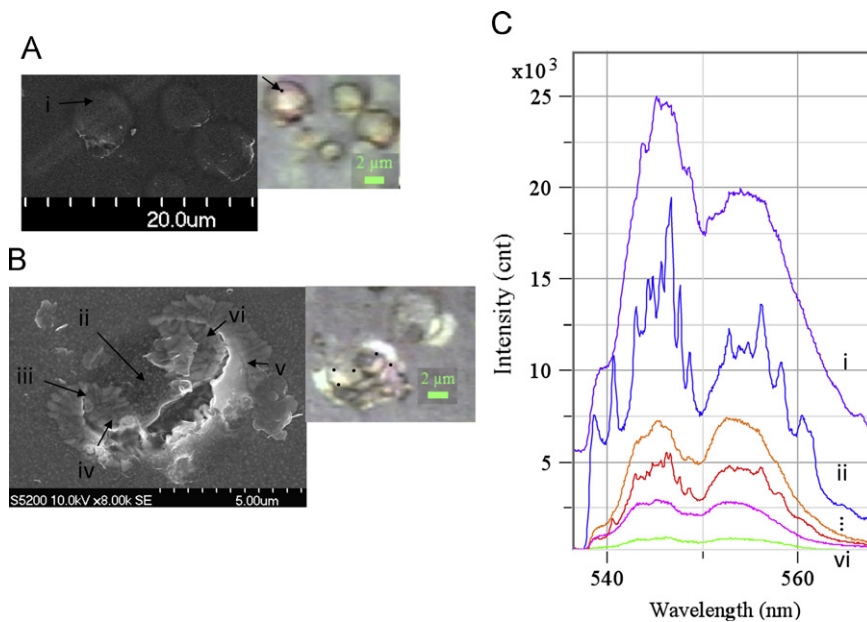


Fig. 6. SEM and optical images of clusters (A, B), with mapped micro-PL spectra (i–vi) shown from top to bottom in (C). Intact regions of thin film exhibit either Type 1 or 2 PL spectra (i, ii, respectively), whereas erbium aggregates exhibit low-intensity in Type 3 spectra (iii–vi). Dots in optical images show original estimates of where the PL laser was focused prior to mapping. With the exception of trace (i), PL spectra in (C) are raw data measured under identical conditions and therefore provide information about the strength of the PL as well as the Stark splitting. It was necessary to scale and shift trace (i) because it was recorded under a different objective.

completely intact and exhibiting a Type 1 PL spectrum. Therefore, the erbium crystalline aggregates are not the source of increased emissions for Type 1 and 2 clusters, but rather these emissions must come from the thin film above the crystals. Likewise, Type 3 clusters measured using PL are clusters that have their erbium aggregate cores exposed from above. In this manner, we examined a total of 13 other clusters, three of which also produced Type 3 spectra emanating from crystalline regions. The remaining 10 clusters had their thin films intact, and exhibited either Type 1 or 2 spectra.

4. Discussion

We have characterized several properties of micrometer-scale clusters that exhibit a substantial increase in PL. To understand the growth of the clusters themselves, it is important to note that the erbium aggregates are not the direct cause of the film's deformation. Fig. 2A clearly shows that there is some space beneath the erbium crystals, which means that they are not directly forcing the film upwards. It is more likely that the thin film has been lifted due to the increased thermal expansion coefficient of the erbium layer ($20.9 \times 10^{-6} \text{ K}^{-1}$ at room temperature) [10] as compared to the fused quartz substrate ($0.55 \times 10^{-6} \text{ K}^{-1}$ at room temperature) [11]. This erbium-rich layer is present throughout the sample, in both the cluster and non-cluster regions (Fig. 2D). Therefore, the clusters may be regions of the thin film that, weakened by the precipitation of erbium, deform as a result of the expanding erbium layer.

To understand the origin of the increased cluster PL, we have shown that it is accompanied by a change in fine structure, which can reflect the local environment of the erbium ions [12]. The observed relationship between fine structure and cluster PL intensity suggests that changes in erbium local environment may be responsible for increases in PL. Additional information about the film can be obtained by examining the fine structure broadening. The fine structure of the non-cluster regions and also of all the three cluster types exhibit underlying broadening that is

characterized by two large peaks centered at 546 and 556 nm (Fig. 4). This underlying broadening is not present in the Er_2O_3 powder and suggests that some of the material in our samples resides in a disordered phase. In contrast, the well-defined peaks riding on top of the Stark spectra in Fig. 4 suggest the coexistence of a more homogenous region as well. Comparing our fine structure measurements to those in the literature shows that our samples contain many peaks that are not reported in the published spectra [13–16]. This is particularly true for Type 2 clusters and also for the non-cluster region. These additional peaks are most likely “hot lines” associated with transitions from higher-energy levels of the excited $^4\text{S}_{3/2}$ state. In the future, low-temperature micro-PL measurements should eliminate these hot lines and allow for classification of the erbium local environment based on the Stark splitting of the $^4\text{I}_{15/2}$ level. This could allow us to identify specific local environments that are associated with the increased PL.

Information about the relationship between cluster formation and the local environment inside the thin film can be gained by studying the erbium-rich globules observed in the SEM images. Since these globules are formed during the annealing process, they should reflect the internal properties of the thin film. However, there is no apparent difference in the size and density of the globules in the cluster centres, versus those in the non-cluster regions. Rather, only at the edges of the cluster there appear any changes in globule size and density. This suggests that cluster formation is accompanied by certain changes in the internal properties of the thin film, such as local changes in stress. However, the localized reduction in globule size does not appear to be caused by the erbium aggregates, which occur throughout the cluster.

There are several possible mechanisms that could explain these findings. Our previous studies have provided evidence that Er^{3+} -related PL emissions in these samples are sensitized by silicon nanocrystals [2], which have been shown to increase the effective cross-section of erbium by up to four orders of magnitude [17]. Thus, a promising hypothesis is that micro-clusters could be sites where the erbium experiences increased

levels of sensitization. This could explain the observed changes in the Stark spectrum, since the incorporation of Er^{3+} ions into the SiO_x matrix that surrounds the silicon nanocrystals would produce changes in the electric fields that the erbium ions perceive [18]. Another possibility is that either the erbium aggregates or smaller particulates of metallic erbium could induce surface-enhanced fluorescence (SEF). SEF occurs when a metallic surface alters the local environment of the fluorescent ions, thereby increasing the ratio of radiative to non-radiative decay. This is often reflected by a reduced fluorescence lifetime and an increased quantum efficiency. Therefore, micro-PL lifetime measurements could be used to test this mechanism.

In addition to low-temperature micro-PL and micro-PL lifetime measurements, several other additional characterizations will help elucidate the underlying mechanisms. Of particular interest is EXAFS (Extended X-ray Absorption Fine Structure), which can provide information about the first and second nearest neighbors [12]. HRTEM (high-resolution transmission electron microscopy) and STEM/EDX (scanning transmission electron microscopy) can provide information about the elemental composition of micro-clusters on much smaller length scales and therefore can identify whether clusters exhibit differences in nanocrystal formation and Er–Si co-localization.

5. Conclusion

We have demonstrated the presence of novel micrometer-scale clusters in our thin film and have shown that these micro-clusters are displaced, partially hollow regions with erbium-rich crystalline aggregates embedded inside. Top-down PL measurements have shown that these clusters exhibit PL that is much stronger than the non-cluster region and significantly exceeds that from Er_2O_3 powder. Thus, with refinement, these clusters could potentially serve as localized emission sources for use in devices.

To further investigate the mechanism of PL enhancement, we have successfully incorporated SEM-mapping into our micro-PL analysis, which is a useful tool for studying samples that are inhomogeneous on the micrometer-scale. From this analysis we have observed that the PL comes from the thin film and not directly from the erbium aggregates. Finally, high resolution PL analysis has shown a distinct correlation between micro-cluster PL intensity and Stark splitting, indicating that the changes in the

local environment of the erbium may produce the enhanced erbium PL.

Acknowledgements

This work was supported by Natural Sciences and Engineering Research Council of Canada (NSERC), the Ontario Centres of Excellence, and the Ontario Research Fund—Research Excellence Program. The authors are grateful to Dr. D. Yeghikyan for help with sample preparation; Dr. N. Coombs and Dr. I. Gourevich for help with SEM/EDX analysis; Dr. V. Venkataramanan for collaboration in micro-PL measurements; Keith Leong for insightful discussions; and Pengpeng Cao, Ernest Ho and Janet Stanley for proofreading the manuscript.

References

- [1] A.J. Kenyon, *Semiconductor Science and Technology* 20 (2005) R65.
- [2] H. Alizadeh, W. Shams-Kolahi, L. Qian, N.P. Kherani, S. Zukotynski, *Japanese Journal of Applied Physics* 47 (9) (2008) 7211.
- [3] J.B. Ainslie, *Journal of Lightwave Technology* 9 (2) (1991) 220.
- [4] S. Colin, E. Contesse, P. Le Boudec, G. Stephan, F. Sanchez, *Optics Letters* 21 (24) (1996) 1987.
- [5] H.L. An, E.Y.B. Pun, X.Z. Lin, H.D. Liu, *IEEE Photonics Technology Letters* 11 (7) (1999) 803.
- [6] G. Wora Adeola, O. Jambois, P. Miska, H. Rinnert, M. Vergnat, *Applied Physics Letters* 89 (2006) 101920.
- [7] M. Wojdak, M. Klik, M. Forcales, O.B. Gusev, T. Gregorkiewicz, *Physical Review B* 69 (2004) 233315.
- [8] C.Y. Cheng, W.D. Chen, S.F. Song, Z.J. Xu, X.B. Liao, G.H. Li, K. Ding, *Journal of Applied Physics* 94 (9) (2003) 5599.
- [9] A. Polman, *Journal of Applied Physics* 82 (1997) 1.
- [10] David R. Lide (Ed.), *Physical Constants of Clear Fused Quartzin: CRC Handbook of Chemistry and Physics, 89th Edition (Internet Version 2009)*, CRC Press/Taylor and Francis, Boca Raton, FL.
- [11] David R. Lide (Ed.), *Room Temperature Coefficient of Thermal Expansion, Thermal Conductivity, Electrical Resistance, and Hall Coefficientin: CRC Handbook of Chemistry and Physics, 89th Edition (Internet Version 2009)*, CRC Press/Taylor and Francis, Boca Raton, FL.
- [12] H. Isshiki, A. Polman, T. Kimura, *Journal of Luminescence* 102 (2003) 819.
- [13] J.D. Carey, R.C. Barklie, J.F. Donegan, *Physical Review B* 59 (4) (1999) 2773.
- [14] N.Q. Vinh, H. Przybylinska, Z.F. Krasil'nik, T. Gregorkiewicz, *Physical Review B* 70 (2004) 115332.
- [15] N.Q. Vinh, H. Przybylinska, Z.F. Krasil'nik, T. Gregorkiewicz, *Physical Review B* 90 (6) (2003) 066401.
- [16] A. Kasuya, M. Suezawa, *Applied Physics Letters* 71 (19) (1997) 2728.
- [17] A.J. Kenyon, C.E. Chryssou, C.W. Pitt, *Journal of Applied Physics* 91 (1) (2002) 367.
- [18] F. Lucarz, A.J. Kenyon, *Silicon nanocrystals in erbium-doped silica for optical amplifiers*, MSc Thesis, University College of London, 2003, pp. 21–23.